16th Mediterranean Conference on Control and Automation
Congress Centre, Ajaccio, France
June 25-27, 2008

Robust Sliding Mode Control of a DFIG Variable Speed Wind Turbine for Power Production Optimization

Boubekeur Boukezzar and Mohamed M'Saad

Abstract— **A cascaded nonlinear sliding mode controller is proposed for power production optimization of a variable speed wind turbine equipped with a Doubly Fed Induction Generator (DFIG). The inner loop controller ensures a robust tracking of both generator torque and rotor flux, while the outer loop controller achieves a robust tracking of the optimal blade rotor speed to optimize wind energy capture.**
The global controller is firstly tested with a simplified mathematical model of the aeroturbine and DFIG for a high-turbulence wind speed profile. Secondly, the aeroturbine controller is validated upon a flexible wind turbine simulator. The obtained results show better performance in comparison with the existing controllers in presence of parameters variations.

Index Terms— **DFIG, nonlinear control, sliding mode, variable speed wind turbines.**

I. Introduction

Wind energy conversion systems (WECS) have quickly evolved over the last decades and efficient and reliable exploitation tools have been developed to make these installations more profitable [1]. Modern high-power wind turbines (WT) are equipped with adjustable speed generators [2]. The doubly fed induction generator (DFIG) with a power converter is a common and efficient configuration to transfer the mechanical energy from the variable speed rotor to a constant frequency electrical grid [3]. Many contributions have been devoted to the control of the aeroturbine mechanical as well as the electrical components [4]. The control objective consists mainly in optimizing the extracted aerodynamic power in partial load area. The control design is generally based on a linearized model of the WT around its operating points [5]. For the DFIG control, classical control techniques as vector control [6] were extensively used. Some nonlinear controllers were proposed assuming that the wind turbine operates in steady state conditions [7]–[9]. The nonlinear dynamical nature of the wind and the turbine is not taken into account. Furthermore, as these nonlinear control techniques are almost parameters dependent, they are indeed affected by the parameters deviations.
The objective of this work is to design two cascaded nonlinear robust controllers for the wind turbine. The first one concerns the aeroturbine, while the second one is devoted to the DFIG. These controllers are designed using the dynamical features of the wind speed, the aeroturbine and the DFIG together with their non-linear characteristics. They must stand robust under parameters variations.

The authors are with the GREYC Control Team, 6 bd du Maréchal Juin, F-14050 Caen, cedex France.
E-mail : boubekeur.boukhezzar, msaad@greyc.ensicaen.fr
Tel :+33 (0)2 31 45 27 14, Fax : +33 (0)2 31 56 73 30.

This paper is organized as follows : The wind turbine and DFIG nonlinear mathematical models are presented in the section II. The control objectives are briefly reminded in section III. Section IV is concerned with the DFIG control, namely the nonlinear input-output linearization and sliding mode controllers. The aeroturbine linearizing and sliding mode controllers are developed in section V according to the required specifications. Simulation results, using a realistic wind turbine simulator, are given in section VI to show the effectiveness of the proposed sliding mode control with respect to the nonlinear input-output linearization control.

II. Wind Turbine Modelling

A. Aeroturbine modelling

The aerodynamic torque expression is given by

$$T_a = \frac{1}{2}\rho\pi R^3 C_q(\lambda,\beta)v^2 \tag{1}$$

The torque coefficient C_q depends on the blade pitch angle β and the tip-speed ratio λ which is defined as follows

$$\lambda = \frac{\omega_t R}{v} \tag{2}$$

where ω_t is the rotor speed R is the rotor radius and ρ is the air density.
As the low-speed shaft is assumed to be perfectly rigid, a single mass model of the turbine may then be considered [10]

$$J_{t_{hs}}\dot{\omega}_g = T_{a_{hs}} - K_{t_{hs}}\omega_g - T_{em} \tag{3}$$

$J_{t_{hs}}$, $K_{t_{hs}}$ and $T_{a_{hs}}$ are respectively the total inertia, external damping and aerodynamic torque brought to the high-speed side. The reader is referred to [10], [11] for more details about aeroturbine modelling and parameters values.

B. DFIG modelling

The DFIG mathematical model can be described by the following nonlinear state space representation. The electrical variables are considered in a $d-q$ reference frame fixed to the stator. The system is a MIMO affine-input nonlinear one.

$$\begin{cases} \dot{\boldsymbol{x}} = \boldsymbol{f}(\boldsymbol{x}) + \boldsymbol{g}\boldsymbol{u}_r + \boldsymbol{d_1}\boldsymbol{u}_s + \boldsymbol{d_2}T_{a_{hs}} \\ \boldsymbol{y} = \boldsymbol{h}(\boldsymbol{x}) \end{cases} \tag{4}$$

where

$$\boldsymbol{x} = \begin{bmatrix} i_{sd} & i_{sq} & \phi_{rd} & \phi_{rq} & \omega_g \end{bmatrix}^T \quad ; \quad T_{a_{hs}} = \frac{T_a}{n_g}$$

$$\boldsymbol{u_s} = \begin{bmatrix} u_{sd} & u_{sq} \end{bmatrix}^T \quad ; \quad \boldsymbol{u_r} = \begin{bmatrix} u_{rd} & u_{rq} \end{bmatrix}^T$$

978-1-4244-2505-1/08/$20.00 ©2008 IEEE

and

$$\boldsymbol{f}(\boldsymbol{x}) = \begin{bmatrix} f_1(x) \\ f_2(x) \\ f_3(x) \\ f_4(x) \\ f_5(x) \end{bmatrix} = \begin{bmatrix} a_{11}x_1 + a_{13}x_3 + a_{14}x_4x_5 \\ a_{11}x_2 + a_{13}x_4 - a_{14}x_3x_5 \\ a_{31}x_1 + a_{33}x_3 + a_{34}x_4x_5 \\ a_{31}x_2 + a_{33}x_4 - a_{34}x_3x_5 \\ a_{51}(x_2x_3 - x_1x_4) + a_{55}x_5 \end{bmatrix}$$

with

$$a_{11} = -\left(\frac{1}{T_s\sigma} + \frac{1}{T_r}\frac{1-\sigma}{\sigma}\right) \quad a_{13} = \frac{1-\sigma}{\sigma}\frac{1}{MT_r} \quad a_{14} = \frac{1-\sigma}{\sigma}\frac{p}{M}$$
$$a_{31} = \frac{M}{T_r} \quad a_{33} = -\frac{1}{T_r} \quad a_{34} = -p$$
$$a_{51} = p\frac{M}{J_{t_{hs}}L_r} \quad a_{55} = \frac{-K_{t_{hs}}}{J_{t_{hs}}}$$

and

$$\boldsymbol{g} = \begin{bmatrix} b_1 & 0 \\ 0 & b_1 \\ 1 & 0 \\ 0 & 1 \\ 0 & 0 \end{bmatrix} \; ; \; \boldsymbol{d_1} = \begin{bmatrix} b_2 & 0 \\ 0 & b_2 \\ 0 & 0 \\ 0 & 0 \\ 0 & 0 \end{bmatrix} \; ; \; \boldsymbol{d_2} = \begin{bmatrix} 0 \\ 0 \\ 0 \\ 0 \\ b_3 \end{bmatrix}$$

with

$$b_1 = -\frac{M}{\sigma L_r L_s} \quad ; \quad b_2 = \frac{1}{\sigma L_s} \quad ; \quad b_3 = \frac{1}{J_{t_{hs}}}$$

R_s and R_r are respectively the stator and rotor resistance, L_s, L_r and M the stator leakage, rotor leakage and mutual inductances. $\sigma = 1 - \dfrac{M^2}{L_r L_s}$ is the scattering coefficient, T_s and T_r are the stator and rotor time constants. p is the number of pole pairs.

The control inputs are the DFIG rotor voltages $\boldsymbol{u_r}$ in the $d-q$ reference frame. The stator voltages and aerodynamic torque can be viewed as uncontrolled inputs.

The two outputs are the rotor flux squared modulus and the electromagnetic torque

$$\boldsymbol{y} = \begin{bmatrix} h_1(x) \\ h_2(x) \end{bmatrix} = \begin{bmatrix} |\phi_r|^2 \\ T_{em} \end{bmatrix} = \begin{bmatrix} x_3^2 + x_4^2 \\ \mu\,(x_1x_4 - x_2x_3) \end{bmatrix}$$

where $\mu = p \cdot \frac{M}{L_r}$.

The used DFIG parameters corresponds to a 660 kW nominal power and are referenced in [12].

III. Control Problem Formulation

A. Control objectives

The aerodynamic power captured by the aeroturbine rotor is given by

$$P_a = \frac{1}{2}\rho\pi R^2 C_p(\lambda,\beta)v^3 \tag{5}$$

The $C_p(\lambda,\beta)$ curve is specific for each wind turbine. It has a unique maximum $C_{p_{opt}}$ at a single point

$$C_p(\lambda_{opt},\beta_{opt}) = C_{p_{opt}} \tag{6}$$

In order to maintain λ at its optimal value for a given wind speed v, the rotor speed must be adjusted using the generator torque to track the reference $\omega_{t_{opt}} = \frac{\lambda_{opt}}{R}v$.

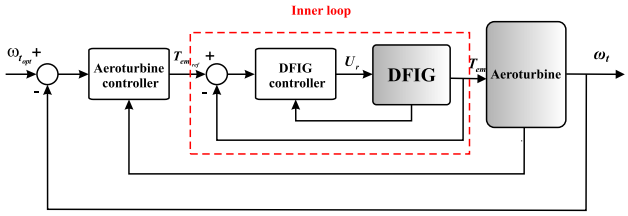

Fig. 1. Wind Turbine Control scheme

The system output to be controlled is the rotor speed ω_t and the control problem is the tracking of an optimal rotor speed reference $\omega_{t_{opt}}$ that ensures maximum wind power capture. Notice that the blade pitch angle could be used as an additional control input to achieve electrical power regulation, for high wind speeds.

B. Control Structure

The WT electric system time responses are much faster than those of the other parts of the WT (Fig. 1). This makes it possible to dissociate the generator and the aeroturbine control designs and thus define a cascaded control structure around two control loops.

1) The inner control loop concerns the electric generator via the power converters.
2) The outer control loop concerns the aeroturbine that provides the reference inputs of the inner loop.

IV. DFIG Robust Control

A. Input-Output Feedback Linearization

We will first assume the system is perfectly modeled.The input-output decoupling linearization is then performed via a nonlinear state feedback.

The notation $L_f h(x)$ is used for the Lie derivative of the output function $h(x)$ along the vector field $f(x)$ and is defined as

$$L_f h(x) = \sum_{i=1}^{n} \frac{\partial h}{\partial x_i} \cdot f_i(x) \tag{7}$$

As $L_{d_2}h_1 = L_{d_2}h_2 = 0$, the first time derivative of the outputs can be written as

$$\begin{bmatrix} \dot{y}_1 \\ \dot{y}_2 \end{bmatrix} = \begin{bmatrix} L_f h_1 \\ L_f h_2 \end{bmatrix} + \boldsymbol{D_r}\begin{bmatrix} u_{rd} \\ u_{rq} \end{bmatrix} + \boldsymbol{D_s}\begin{bmatrix} u_{sd} \\ u_{sq} \end{bmatrix} \tag{8}$$

where

$$\begin{cases} L_f h_1 &= 2(a_{31}(x_1x_3 + x_2x_4) + a_{33}\,|\phi_r|^2) \\ L_f h_2 &= (a_{11} + a_{33})T_{em} + \\ & \quad \mu(-a_{34}(x_1x_3 + x_2x_4) + a_{14}\,|\phi_r|^2)x_5 \end{cases}$$

$$\boldsymbol{D_r} = \begin{bmatrix} L_{g_1}h_1 & L_{g_2}h_1 \\ L_{g_1}h_2 & L_{g_2}h_2 \end{bmatrix} = \begin{bmatrix} 2x_3 & 2x_4 \\ \mu(b_1x_4 - x_2) & \mu(x_1 - b_1x_3) \end{bmatrix}$$

and

$$\boldsymbol{D_s} = \begin{bmatrix} L_{d_{11}}h_1(x) & L_{d_{12}}h_1(x) \\ L_{d_{11}}h_2(x) & L_{d_{12}}h_2(x) \end{bmatrix} = \begin{bmatrix} 0 & 0 \\ \mu b_2 x_4 & -\mu b_2 x_3 \end{bmatrix}$$

Choosing

$$\begin{bmatrix} u_{rd} \\ u_{rq} \end{bmatrix} = -D_r^{-1} \cdot \left[\begin{bmatrix} L_f h_1 \\ L_f h_2 \end{bmatrix} + D_s \begin{bmatrix} u_{sd} \\ u_{sq} \end{bmatrix} - \begin{bmatrix} v_1 \\ v_2 \end{bmatrix} \right] \quad (9)$$

equation (8) is reduced to the linearized and decoupled system

$$\begin{bmatrix} \dot{y}_1 \\ \dot{y}_2 \end{bmatrix} = \begin{bmatrix} v_1 \\ v_2 \end{bmatrix} \quad (10)$$

To ensure a first order tracking dynamic of the squared rotor flux $|\phi_r|^2$ and electromagnetic torque reference $T_{em_{ref}}$ references, the new control inputs v_1 and v_2 are given by

$$\begin{aligned} v_2 &= -l_2(|\phi_r|^2 - \Phi_r) + \dot{\Phi}_r \\ v_1 &= -l_1(T_{em} - T_{em_{ref}}) + \dot{T}_{em_{ref}} \end{aligned} \quad (11)$$

where l_1 and l_2 are constants that determine the tracking dynamic.

B. Nonlinear Sliding Mode control

In presence of modelling uncertainties, a robust controller is needed to achieve a high-performance control.
Let us introduce the control vector surface $\boldsymbol{S} = [s_1 \quad s_2]^T$ defined by :

$$\begin{cases} s_1 = & |\phi_r|^2 - \Phi_r = y_1 - y_{1_{ref}} \\ s_2 = & T_{em} - T_{em_{ref}} = y_2 - y_{2_{ref}} \end{cases} \quad (12)$$

Defining

$$\boldsymbol{f}^* = \begin{bmatrix} L_f h_1 \\ L_f h_2 \end{bmatrix} + \boldsymbol{D_s} \begin{bmatrix} u_{sd} \\ u_{sq} \end{bmatrix}$$

equation (8) can be rewritten as

$$\dot{\boldsymbol{y}} = \boldsymbol{f}^*(\boldsymbol{x}) + \boldsymbol{D_r}\boldsymbol{u_r} \quad (13)$$

If we assume that the parametric uncertainties on the DFIG model parameters are gathered in the functions $\boldsymbol{f}^*$ and $\boldsymbol{D_r}$ and satisfy the fellowing bounds

$$\begin{aligned} &\left| f_i^*(\boldsymbol{x}) - \hat{f}_i^*(\boldsymbol{x}) \right| \le \delta_i \\ &\boldsymbol{D_r} = (I + \boldsymbol{\Delta})\hat{\boldsymbol{D}}_{\boldsymbol{r}}, \quad \left|\Delta_{ij}\right| \le D_{ij} \end{aligned} \quad (14)$$

By choosing the Lyapunov function

$$V = \frac{1}{2}\boldsymbol{S}^T\boldsymbol{S} = \frac{1}{2}\sum_{i=1}^{2} s_i^2 \quad (15)$$

The control inputs $\boldsymbol{u_r}$ are then chosen in order to satisfy the sufficient conditions for the existence and reachability of a sliding mode [13] :

$$s_i \dot{s}_i \le -\eta_i |s_i|, \ \ i = 1,2. \quad (16)$$

where $\boldsymbol{\eta} = [\eta_1 \quad \eta_2]^T$ are positive constants.
The proposed sliding mode controller is composed of a nominal part and an additional terms to handle model uncertainties

$$\boldsymbol{u_r} = \hat{\boldsymbol{D}}_{\boldsymbol{r}}^{\ -1} \cdot \left[\dot{\boldsymbol{y}}_{ref} - \hat{\boldsymbol{f}}^*(\boldsymbol{x}) - \boldsymbol{K} \cdot \times sgn(\boldsymbol{S}) \right] \quad (17)$$

where the operators $sgn(.)$ and $\cdot\times$ are defined as [14]

$$\begin{aligned} sgn(\boldsymbol{S}) &= \begin{bmatrix} sgn(s_1) & sgn(s_2) \end{bmatrix}^T \\ \boldsymbol{x} \cdot \times \boldsymbol{y} &= [x_1 \cdot y_1, x_2 \cdot y_2, \cdots, x_n \cdot y_n] \end{aligned}$$

and

$$\boldsymbol{K} = \begin{bmatrix} k_1 & k_2 \end{bmatrix}^T$$

From (15),

$$\dot{V} = s_1 \cdot \dot{s}_1 + s_2 \cdot \dot{s}_2$$

substituting (13) in s_1 and s_2 time derivatives obtained from (12) yields

$$\begin{cases} \dot{s}_1 = f_1^* - \hat{f}_1^* + \sum_{j=1}^{2} \Delta_{1j}(\dot{y}_{j_{ref}} - \hat{f}_j^*) - \Delta_{12}k_2 \mathrm{sgn}(s_2) \\ \qquad -(1+\Delta_{11})k_1 \mathrm{sgn}(s_1) \\ \dot{s}_2 = f_2^* - \hat{f}_2^* + \sum_{j=1}^{2} \Delta_{2j}(\dot{y}_{j_{ref}} - \hat{f}_j^*) - \Delta_{21}k_1 \mathrm{sgn}(s_1) \\ \qquad -(1+\Delta_{22})k_2 \mathrm{sgn}(s_2) \end{cases}$$

From the above equations, as $\left| f_i^*(\boldsymbol{x}) - \hat{f}_i^*(\boldsymbol{x}) \right| \le \delta_i$ and $\left|\Delta_{ij}\right| \le D_{ij}$ for $i = 1,2$, to satisfy the existence and reachability condition (16), the gains k_1, k_2 in (17) must verify the following inequalities [15], [14].

$$\begin{aligned} s_1\dot{s}_1 \le \quad & |s_1| \cdot \left[\delta_1 + \sum_{j=1}^{2} D_{1j} \cdot \left| \dot{y}_{j_{ref}} - \hat{f}_j^* \right| \right. \\ & \left. -D_{12} \cdot k_2 - (1 - D_{11})k_1 \right] \le -\eta_1 \cdot |s_1| \end{aligned} \quad (18)$$

$$\begin{aligned} s_2\dot{s}_2 \le \quad & |s_2| \cdot \left[\delta_2 + \sum_{j=1}^{2} D_{2j} \cdot \left| \dot{y}_{j_{ref}} - \hat{f}_j^* \right| \right. \\ & \left. -D_{21} \cdot k_1 - (1 - D_{22})k_2 \right] \le -\eta_2 \cdot |s_2| \end{aligned} \quad (19)$$

therefore, the condition is verified for all $k_i \ge k_i'$, where $\boldsymbol{K}' = \begin{bmatrix} k_1' & k_2' \end{bmatrix}^T$ satisfies

$$(\boldsymbol{I} - \bar{\boldsymbol{D}})\boldsymbol{K}' = \boldsymbol{\delta} + \boldsymbol{D}\left| \dot{\boldsymbol{y}}_{ref} - \hat{\boldsymbol{f}}^*(\boldsymbol{x}) \right| + \boldsymbol{\eta} \quad (20)$$

with,

$$\boldsymbol{D} = \begin{bmatrix} D_{11} & D_{12} \\ D_{21} & D_{22} \end{bmatrix} ; \bar{\boldsymbol{D}} = \begin{bmatrix} D_{11} & -D_{12} \\ -D_{21} & D_{22} \end{bmatrix}$$

According to Frobenius-Perron theorem [15], equation (20) has a solution and all k_i' are all positive.
As condition (16) holds, one has $|S| \to 0$ and hence $T_{em} \to T_{em_{ref}}$ and $|\phi_r|^2 \to \Phi_r$ thanks to Barbalat's Lemma [16].

V. Aeroturbine Robust Control

A. Nonlinear static feedback linearization with asymptotic rotor speed reference tracking

In order to design a high-level controller of the aeroturbine, it is more convenient to consider the one mass model where all the inertias are transferred to the low speed shaft [17].

$$J_t \dot{\omega}_t = T_a - K_t \omega_t - T_g \quad (21)$$

A first order dynamic response is selected for the rotor speed tracking error as follows

$$\dot{\varepsilon} + a_0 \varepsilon = 0 \ , \quad a_0 > 0 \quad (22)$$

where $\varepsilon = \omega_{t_{opt}} - \omega_t$.
As mentioned in [18], this is achieved by imposing the fellowing control torque

$$T_g = T_a - K_t\omega_t - J_t a_0 \varepsilon - J_t \dot{\omega}_{t_{opt}} \tag{23}$$

This technique has been shown to lack robustness with respect to parameters uncertainties [15], so a nonlinear sliding mode controller is developed next.

B. Nonlinear Sliding Mode control

Defining a third sliding surface

$$s_3 = \omega_t - \omega_{ref}$$

it comes from (21) that

$$\dot{s}_3 = f_6 - \frac{1}{J_t} T_g - \dot{\omega}_{ref} \tag{24}$$

where $f_6 = \dfrac{1}{J_t}\left[T_a - K_t\omega_t\right]$
By choosing the generator torque

$$T_g = \hat{J}_t \cdot \left[\hat{f}_6 - \dot{\omega}_{ref} + a_0(\omega_t - \omega_{ref}) + k_3 \mathrm{sgn}(s_3)\right] \tag{25}$$

(24) is rewritten as

$$\begin{aligned} \dot{s}_3 \quad = \quad & (f_6 - \frac{\hat{J}_t}{J_t}\hat{f}_6) - (1 - \frac{\hat{J}_t}{J_t})\dot{\omega}_{ref} - \frac{\hat{J}_t}{J_t} a_0(\omega_t - \omega_{ref}) \\ & - \frac{\hat{J}_t}{J_t} k_3 \cdot \mathrm{sgn}(s_3) \end{aligned} \tag{26}$$

The reachability condition

$$s_3 \cdot \dot{s}_3 \leq -\eta \cdot |s_3| \tag{27}$$

holds for all k_3 satisfying,

$$k_3 \geq \left| \frac{J_t}{\hat{J}_t} f_6 - \hat{f}_6 - \left(\frac{J_t}{\hat{J}_t} - 1\right) \dot{\omega}_{ref} - a_0\left(\omega_t - \omega_{ref}\right) \right| + \eta \cdot \frac{J_t}{\hat{J}_t}$$

Assuming,

$$\left|f_6 - \hat{f}_6\right| = \left| \frac{1}{J_t}\left[T_a - K_t\omega_t\right] - \frac{1}{\hat{J}_t}\left[\hat{T}_a - \hat{K}_t\omega_t\right] \right| \leq \delta_6$$

and by setting $\kappa = \dfrac{J_t}{\hat{J}_t}$, the control law (25) ensures a robust tracking of the optimal rotor speed for all k_3 verifying

$$k_3 \geq \kappa\delta_3 + \eta\kappa + |\kappa - 1| \cdot \left|\hat{f}_6 - \dot{\omega}_{ref}\right| + a_0 \cdot \left|\omega_t - \omega_{ref}\right| \tag{28}$$

VI. SIMULATION RESULTS

The numerical simulations were performed on a wind turbine whose characteristics can be found in [12], [17]. These parameters correspond to the Controls Advanced Research Turbine (CART) which is located at NREL. The CART is a variable-speed, variable pitch WT with a nominal power rating of 600 kW and a hub height of 36 m. It is a 43-m diameter, 2-bladed, teetered hub machine. It is assumed to be coupled to a three-phase DFIG. Its characteristics are given in the same table. This turbine was modelled with the mathematical model and the FAST (Fatigue, Aerodynamics, Structures and Turbulence) aeroelastic simulator for validation. FAST code is developed by NREL [19]. It is capable of modeling two and three bladed propeller-type machines.

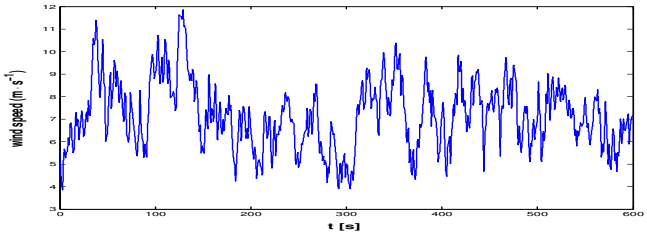

Fig. 2. Wind speed profile of 7 $\mathrm{m \cdot s^{-1}}$ mean value.

TABLE I
AEROTURBINE SLIDING MODE CONTROLLER PERFORMANCE FOR DIFFERENT WIND SPEED PROFILES

Mean wind speed	Efficiency [%]	T_{hs} standard deviation [kN.m]	max T_g [kN.m]
7 m/s	70.41	14.05	73.88
8 m/s	69.79	17.50	84.75
8.5 m/s	69.33	18.29	100.03

A. Using the simplified mathematical model

The proposed cascade control performances are firstly tested using the simplified one-mass mathematical model with the DFIG. All stator and rotor resistances R_r and R_s are increased respectively by an amount of 50 %. The DFIG control system performances are firstly investigated. In order to reduce chaterring phenomenon and obtain an acceptable control loads, the signum function in the control laws is replaced by a smooth approximation using a hyperbolic tangent sigmoid function. Though, this function does not achieve a zero tracking error, it gives a good compromise between chattering reduction and reference tracking.
As seen in Fig. 3(a), the rotor squared flux $|\phi_r|^2$ reach the constant desired reference Φ_r in less than 2 s. Despite the parameters uncertainties, the maximal tracking errors remain acceptable. The DFIG torque T_{em} is then independently controlled to track the reference torque $T_{em_{ref}}$. The torque controller achieves a good performance while T_{em} and $T_{em_{ref}}$ are practically confused (Fig. 3(b)).
For the aeroturbine control system testing, the aeroturbine rotor inertia J_t an damping K_t are also increased by an amount of 50 %. Fig. 4(a) shows the blade rotor speed ω_t tracks the mean tendency of the optimal rotational speed $\omega_{t_{opt}}$ without tracking the turbulent component. It is worth noticing that this tracking performance has been achieved in the presence of parameter uncertainties. The difference between the rotor speed and its optimal reference appears clearly during the start-up transient. Fig. 4(b) shows that the wind turbine electrical power remain smooth. This is due to the choice of an adapted optimal rotor speed tracking dynamic. The simulation results show that the required performance are reached using the two-levels robust sliding mode controllers.

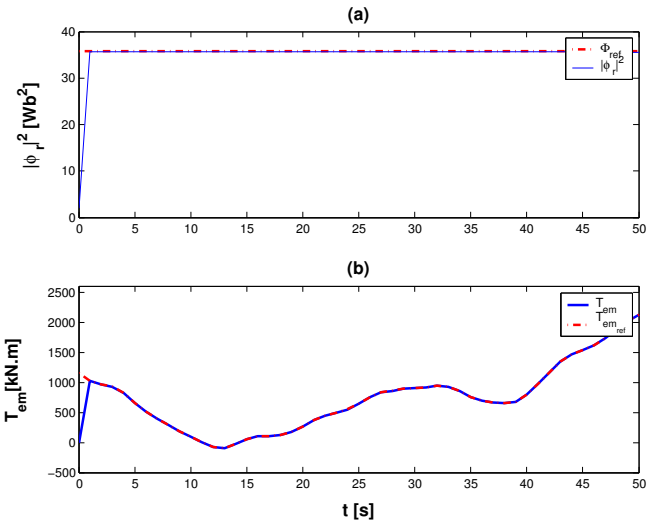

Fig. 3. DFIG Sliding Mode Controller performances

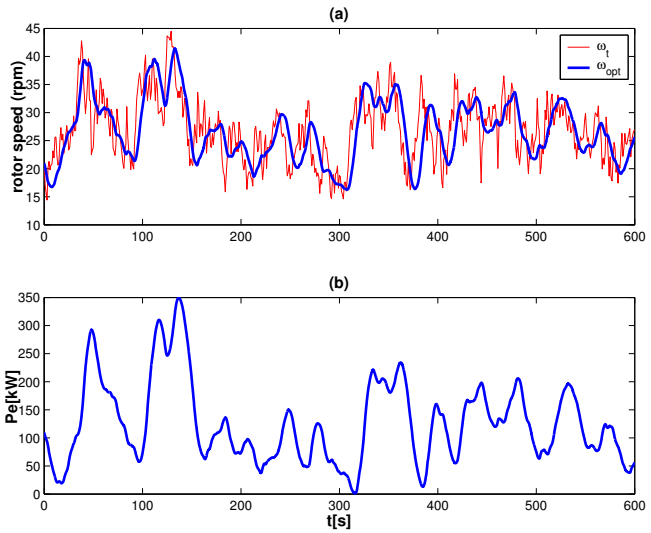

Fig. 4. Aeroturbine Sliding Mode Controller performances

TABLE II

COMPARISON OF THE CONTROL STRATEGIES

Controller	Efficiency [%]	T_{ls} standard deviation [kN.m]	max T_g [kN.m]
Linearizing controller	64.71	12.18	72.12
Sliding mode controller	70.41	14.05	73.88

B. Validation using FAST

The high-level robust sliding mode and linearizing aeroturbine controller were implemented using the FAST flexible aeroturbine simulator. Simulations have been conducted for different wind speed profiles. The controller performance is summarized in TABLE I for different mean wind speeds. Despite the aeroturbine parameters variations, the power capture efficiency remain very good for all wind speed profiles, that is about 70 %. The low speed shaft and generator torque remain also acceptable for all the considered scenarios. Fig. 5 compare the performance obtained using the two controllers in presence of model parameters uncertainties. For the linearizing controller, this causes the deviation of the rotor speed from its optimal reference (Fig. 5(a)). The deviation induce an important power capture loss as shown in Fig. 5(c). One may observe in Fig. 5(b) that the control torque used by the sliding mode controller is more important than that developed by the input output linearizing one. However, it still remains below the upper bound of 162 kN.m. TABLE II summarize the performance of the two controllers. One can see that an increase of 5 % in power capture is achieved thanks to the robustness of the proposed controller. TABLE II and Fig. 5(d) shows that the torque in the low speed shaft remain close for the two controllers.

VII. CONCLUSION

A cascaded nonlinear sliding mode control system is proposed in this work for power production optimization of a variable speed wind turbine equipped with a Doubly Fed Induction Generator.

The controllers guarantees robustness against parameters variations. In presence of rotor and stator resistances uncertainties, the sliding mode DFIG controller achieves a good tracking of rotor reference flux and torque. Similarly, the aeroturbine sliding mode controller ensures a robust tracking of the optimal wind turbine rotor speed in order to maximize the extracted energy from the wind, below the rated power area. This controller has shown better performance than classical approaches in presence of model uncertainties. The validation using an aeroelastic wind turbine simulator justified the efficiency of the proposed approach.

To implement the proposed controllers, discrete time version will be considered in future works. The study of the global stability of the controlled system and the use of higher-order sliding mode controllers are also interesting prospects.

REFERENCES

[1] J. F. Manwell, J. McGowan, and A. Rogers, *Wind Energy Explained : Theory, Design and Applications*. John Wiley & Sons, 2002.

[2] S. Muller, M. Deicke, and R. W. De Doncker, "Doubly fed induction generator systems for wind turbines," *IEEE Industry Application Magazine*, pp. 26–33, May/June 2002.

[3] M. Lindholm, *Doubly Fed Drives for Variable Speed Wind Turbines*. PhD thesis, Technical University of Denmark, 2004.

[4] B. Hopfensberger, D. J. Atkinson, and R. A. Lakin, "Stator flux oriented control of a cascaded doubly-fed induction machine," *IEE Proceedings - Electric Power Applications*, pp. 597–605, 1999.

[5] X. Ma, *Adaptive Extremum Control And Wind Turbine Control*. PhD thesis, Danemark, May 1997.

[6] R. J. Cardenas, R. S. Pena, J. Asher, G. M. Asher, and J. C. Clare, "Sensorless control of a doubly-fed induction generator for stand alone operation," in *IEEE 35th Annual Power Electronics Specialists Conference*, vol. 5, pp. 3378–3383, June 20-25 2004.

[7] Y. D. Song, B. Dhinakaran, and X. Y. Bao, "Variable speed control of wind turbines using nonlinear and adaptive algorithms," *Journal of Wind Engineering and Industrial Aerodynamics*, vol. 85, pp. 293–308, April 2000.

[8] A. Mullane, G. Lightbody, R. Yacamini, and S. Grimes, "Adaptive control of variable speed wind turbines.," in *36th Universities Power Enginering Conference*, (Swansea, UK), 12-24th September 2001.

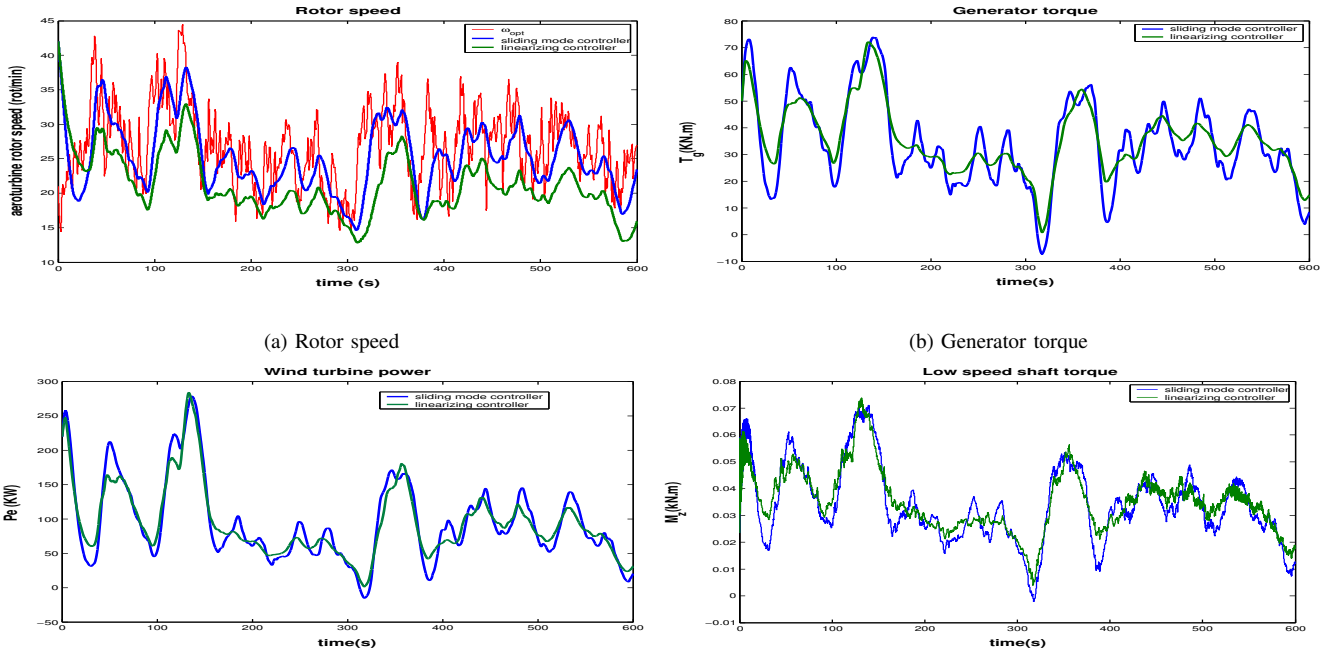

(a) Rotor speed

(b) Generator torque

(c) Electric power

(d) Low speed shaft torque

Fig. 5. Comparison of the aeroturbine control strategies

[9] F. Valenciaga and P. F. Puleston, "Variable structure control of a wind energy conversion system based on a brushless doubly fed reluctance generator," *IEEE Transaction on Energy Conversion*, vol. 22, pp. 499–506, June 2007.

[10] B. Boukhezzar, *Sur les Stratégies de Commande pour l'Optimisation et la Régulation de Puissance des Eoliennes à Vitesse Variable*. PhD thesis, Université de Paris-Sud-Ecole Supérieure d'Electricité, février 2006.

[11] S. E. Aimani, *Modélisation de différentes technologies d'éoliennes intégrées dans un réseau moyenne tension*. PhD thesis, Ecole Centrale de Lille-Université des Sciences et Technologies de Lille 1, december 2004.

[12] Z. M. C. Serban and H. Siguerdidjane, "Direct torque control of a doubly-fed induction generator of a variable speed wind turbine power regulation," in *2007 European Wind Energy Conference Proceedings*, (Milan, Italy), pp. 12–9–138, EWEA, 2007.

[13] R. DeCarlo, S. Zak, and G. Matthews, "Variable structure control of nonlinear multivariable systems : a tutorial," *Proceedings of the IEEE*, vol. 76, pp. 212–232, Mar 1988.

[14] T. I. Fossen and B. A. Foss, "Sliding control of MIMO nonlinear systems," in *European Control Conference*, pp. 12–9–138, 1991.

[15] J. J. E. Slotine and L. Weiping, *Applied Nonlinear Control*. Prentice-Hall, 1990.

[16] J. T. Spooner, M. Maggiore, and R. Ordóñez, *Stable Adaptive Control and Estimation for Nonlinear Systems : Neural and Fuzzy Approximator Techniques*. Wiley-Interscience, 2002.

[17] B. Boukhezzar, H. Siguerdidjane, and M. Hand, "Nonlinear control of variable-speed wind turbines for generator torque limiting and power optimization," *ASME Journal of Solar Energy Engineering*, vol. 128, pp. 516–530, November 2006.

[18] B. Boukhezzar and H. Siguerdidjane, "Nonlinear control of variable speed wind turbines without wind speed measurement," in *ECC-CDC 2005*, (Seville, Spain), 2005.

[19] J. M. Jonkman and M. L. Buhl, *FAST USER's GUIDE*. National Wind Technology Center, National Renewable Energy Laboratory, Golden, Colorado, 6.0 ed., June 2005.